Microwave-free *J*-driven dynamic nuclear polarization: A proposal for enhancing the sensitivity of solution-state NMR

Maria Grazia Concilio * and Lucio Frydman *
Department of Chemical and Biological Physics, Weizmann Institute of Science, Rehovot, Israel

(Received 13 July 2022; revised 1 January 2023; accepted 16 February 2023; published 15 March 2023)

J-driven dynamic nuclear polarization (JDNP) was recently proposed for enhancing the sensitivity of solution-state nuclear magnetic resonance (NMR), while bypassing the limitations faced by conventional (Overhauser) DNP at magnetic fields of interest in analytical applications. Like Overhauser DNP, JDNP also requires saturating the electronic polarization using high-frequency microwaves known to have poor penetration and associated heating effects in most liquids. The present microwave-free JDNP (MF-JDNP) proposal seeks to enhance solution NMR's sensitivity by shuttling the sample between higher and lower magnetic fields, with one of these fields providing an electron Larmor frequency that matches the interelectron exchange coupling J_{ex}. If spins cross this so-called JDNP condition sufficiently fast, we predict that a sizable nuclear polarization will be created without microwave irradiation. This MF-JDNP proposal requires radicals whose singlet–triplet self-relaxation rates are dominated by dipolar hyperfine relaxation, and shuttling times that can compete with these electron relaxation processes. This paper discusses the theory behind the MF-JDNP, as well as proposals for radicals and conditions that could enable this new approach to NMR sensitivity enhancement.

DOI: 10.1103/PhysRevE.107.035303

I. INTRODUCTION

Overhauser dynamic nuclear polarization (ODNP) can enhance the sensitivity of solution-state NMR by saturating an electron radical comixed with the sample of interest [1–3]. However, unless aided by the contact couplings that occasionally arise in the presence of considerable electron delocalization on the target nucleus [4–10], ODNP is only efficient at low magnetic fields [11–16]. High-field ODNP experiments based on inter-molecular contact couplings have thus been reported on nuclei like ^{31}P [17,18], ^{19}F [4,19], and ^{13}C [8,20,21]. However, in more general and analytically relevant cases such as those involving ^{1}Hs, the electron and nuclei will interact solely through intermolecular dipolar couplings. In such systems, where a radical interacts with the solvent only through dipolar couplings, the DNP efficiency decays rapidly with magnetic field B_0. Indeed, typical ^{1}H ODNP enhancements drop from a maximum of $\approx 330\times$ when $B_o \leqslant 0.4$ T, to $\approx 1.001\times$ at the $\geqslant$ 7T fields where contemporary NMR is done [16,20,22–25]. The decreased efficiency of ODNP with magnetic field deprives solution NMR from the benefits that DNP has brought to solid-state analyses [26–29].

We have recently discussed a possible way to bypass these solution-state limitations, based on what we denominate the *J*-driven DNP (JDNP) effect [30]. JDNP requires stable biradicals with identical monomers and an interelectron exchange coupling J_{ex} close to the electron Larmor frequency ω_E. As the JDNP condition $J_{ex} \approx \pm\omega_E$ is fulfilled, a difference between the relaxation rates for the two-electron singlet and triplet states which are dipolar (hyperfine) coupled to the nuclear α or β states can lead, upon electron irradiation, to a transient imbalance between these nuclear populations. This in turn leads to a nuclear magnetization enhancement. The physics of JDNP is reminiscent of that observed in chemically induced dynamic nuclear polarization (CIDNP) [31–36], an experiment in which a laser or a chemical reaction will drive the system away from the thermal equilibrium. The main JDNP requirements are thus stable biradicals, an interelectron J_{ex} on the order of ω_E, and an efficient microwave irradiation at the electron Larmor frequency. Many radicals groups could serve as the starting point for the synthesis of such biradicals, whose J_{ex} would have to reach into the 100s of GHz [37–39]. Exchange couplings in the 90–290 GHz range, for instance, have been obtained by linking bistrityl-based radicals [39].

Electron saturation at such frequencies, however, is problematic in terms of microwave availability, sample heating, and microwave penetration; in fact, even the exact J_{ex} values are hard to predict or measure in solutions. The present study discusses a shuttling-based proposal [40–44] that might bypass these limitations. The ensuing microwave-free JDNP (MF-JDNP) approach proposes to polarize the nuclear spins by shuttling the sample between a lower and a higher magnetic field. Sample-shuttling technologies have been used previously in DNP to enhance ^{13}C signals in experiments involving optical pumped nitrogen-vacancy (NV) centers in diamonds, as well as to increase the ^{1}H and ^{13}C high-field polarization after executing ODNP at low magnetic fields [5,41,45]. In the case of MF-JDNP, we show that if either the starting or the final magnetic field in a two-field shuttling experiment fulfills the $J_{ex} \approx \pm\omega_E$ condition, nuclear polarization will be enhanced by the electrons.

II. SPIN SYSTEMS AND METHODOLOGY

This study's calculations were performed using the SPINACH software package [46] based on laboratory-frame

*Corresponding authors: maria-grazia.concilio@weizmann.ac.il; lucio.frydman@weizmann.ac.il

TABLE I. Biradical spin-system parameters used in the simulations.

Parameter	Spin system
^{1}H chemical shift tensor eigenvalues, [*xx yy zz*], ppm	[5 5 5]
^{1}H chemical shift tensor, *ZYZ* active Euler angles, rad	[0.0 0.0 0.0]
Electron 1 *g*-tensor eigenvalues, [*xx yy zz*], Bohr magneton	[2.0032 2.0032 2.0026]
Electron 1 *g*-tensor, *ZYZ* active Euler angles, rad	[0.0 0.0 0.0]
Electron 2 *g*-tensor eigenvalues, [*xx yy zz*], Bohr magneton	[2.0032 2.0032 2.0026]
Electron 2 *g*-tensor, *ZYZ* active Euler angles, rad	[0.0 0.0 0.0]
^{1}H coordinates [*x y z*]/Å	Solvent ^{1}H in region A: [1.27,1.61,2.26] Solvent ^{1}H in region B: [15.46,10.05,-8.0] Radical proton in region C: [0.0 0.0 10.4]
Electron 1 and electron 2 coordinates, [*x y z*]/Å	[0 0 −7.20] and [0 0 7.20],
Rotational correlation time τ_C/ns	2.2
Scalar relaxation modulation depth/GHz	1
Scalar relaxation modulation time/ps	1
Temperature/K	298

Hamiltonians, as no rotating-frame approximation with respect to the microwaves is *a priori* justified. The simulation code is provided in the Supplemental Material [47]. For simplicity the electron *g*-tensors were assumed identical, axially symmetric, and collinear, as would result from radicals joined by a short, rigid linker; still, as in liquids these *g*-tensors could become noncollinear due to rotational and vibrational modes, the effect of *g*-tensor orientation on the enhancement is discussed in the Supplemental Material [47]. The electrons' relaxation and spin dynamics were described using singlet and triplet basis sets, suitable for this $\Delta\omega \ll J_{ex}$ scenario. Spin-population operators corresponding to the α and β nuclear components of these singlet and the triplet states were considered, and described using Vega's fictitious operators notation [30,48,49]. Three- and four-spin systems were considered, encompassing in all cases the aforementioned two-electron biradical plus protons. One of the protons was always assigned to a fluid medium that would dynamically diffuse around the biradical as described below; this is the "solvent" ^{1}H whose polarization enhancement MF-JDNP is seeking, and which was assumed to interact with the electrons solely through dipolar (also known as anisotropic hyperfine) couplings. Fermi contact couplings were here disregarded; this is justified by the fact that such protons would be located $\geqslant$ 5 Å away from the biradical's main electron density. A second proton with spatial coordinates fixed vs the electrons was occasionally included; the purpose of adding this intraradical ^{1}H was to evaluate the detrimental effect that a proton belonging to the biradical will have on MF-JDNP's ability to polarize the medium. Further details about the assumed systems are given in Table I.

To investigate the physics behind MF-JDNP, brute-force numerical simulations accounting for every self- and cross-relaxation term within the Bloch-Redfield-Wangsness relaxation theory [50–52] were implemented in the SPINACH software [46]. Considering that the exchange coupling has the same order of magnitude as the electron Larmor frequency, these calculations incorporated into the relaxation superoperator a scalar relaxation of the first kind [53]. According to Redfield's relaxation theory, and for the conditions mentioned above, the singlet and triplet-relaxation rates of a biradical with identical *g*-tensors will be dominated by the dipolar hyperfine interactions between the electrons and the surrounding protons [30]. The lifetimes (T_1) for the $\hat{T}_{\pm1,\alpha/\beta}$ states will then vary strongly with the distance between the electrons and the protons: when ^{1}Hs do not approach the biradical electrons to distances closer than 5 Å, these T_1s extend into the ms range [30]; in the presence of "radical" protons sited $\leqslant$ 5 Å away from either of the electrons, these T_1s drop to $\approx$ 100 μs (see Supplemental Material for the relaxation rates predicted by Redfield theory as a function of these and other parameters [47]). This in turn posed the issue of how to estimate the relaxation behavior expected from two electrons interacting with solvent protons, which can take a number of distances from the electrons.

Figure 1 presents the model used to reproduce the expected behavior. Overall, we found that three regions can be distinguished for the behavior of these protons (*vide infra*). There is a "polarizing" region active when electron-nuclear distances are $\sim$ 5–10 Å (labeled "A" in Fig. 1), where the JDNP is active and also relaxation times are short. Then there is an "outer" region arising when the ^{1}H is $\geqslant$ 10 Å away from the closest electron (labeled "B" in Fig. 1), in which the nucleus will not undergo polarization enhancement, and electrons will only contribute to speed up the nuclear relaxation. This B region extends until the protons fall under the influence of another biradical, which for prototypical concentrations ($<$ 10 mM) will be sited some 30 Å away from the original biradical. Finally, there is a "close-contact" region (labeled "C" in Fig. 1) in which protons from the biradical itself reside, and which solvent protons will not be able to penetrate.

In the case of a solvent proton, the nuclear spin will be diffusing randomly at $\approx$ 1 μm^2/ms ($\approx 10^{-9}$ m^2 s^{-1} diffusivity constant [11]), crossing several times in-and-out regions in which JDNP is active and regions where it is not. To account for this in our calculations, a periodic box of size 30×30×30 Å^3 centered on a biradical was established, and a set of ten random walks in this 3D space were executed while counting how often the solvent proton diffuses in and out between the polarizing (A) and nonpolarizing (B) regions to which it was allowed. Figure 1 shows an example

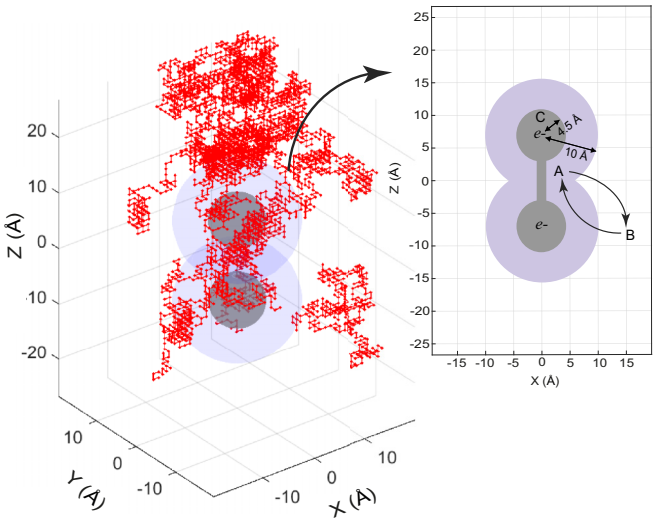

FIG. 1. Example of random walks undertaken by a nuclear "solvent" spin with in a 3D box with a size equal to 30×30×30 Å^3, with a diffusion constant of 1 μm^2/ms, corresponding to a random walk of 10000 steps of 1 Å in 1 ms. Periodic boundary conditions were set to represent an infinite system in which the nuclear spin can get out from a side of the box and get in from the other. Inset: Polarization region accessible by the solvent (violet region) surrounding the biradical (gray circles connected by a linker). A and B represent proton configurations inside and outside of the polarization region, respectively; C represents an intra-radical proton. Representative particles' coordinates are as given in Table I. The code used to perform this random walk is provided in the Supplemental Material [47].

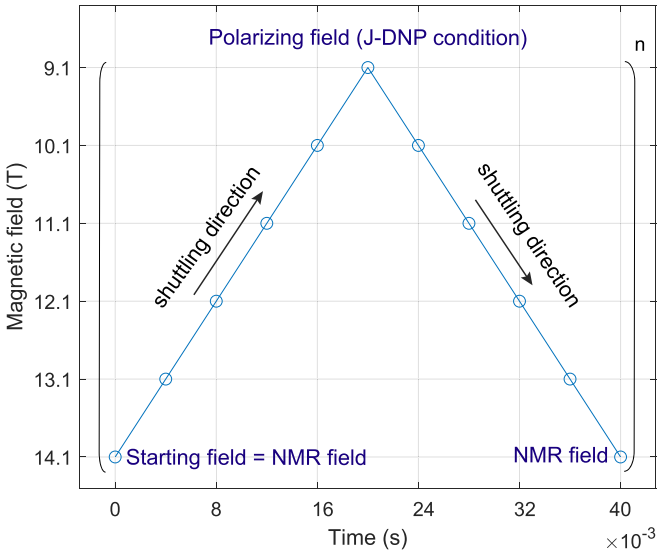

FIG. 2. Schematic description of the high→low→high B_0-cycling in MF-JDNP, in which the sample is shuttled n times at constant 0.25 T/ms rates from a starting magnetic field to a lower field corresponding to the JDNP condition, and then back to the NMR field in which the measurement is performed.

of such walks, which reveal that on average a nuclear spin will spend about 10% of its time within the polarizing region A, and the remaining 90% of its time in the outer, nonpolarizing region B. To account for this constant interruption of the polarization process in the simulations, we set up a randomized polarizing scheme where proton coordinates were constantly exchanged between regions A and B, with time steps of 1×10^{-6} and 9×10^{-6} s, respectively. Within each of these regions the total electron-nuclear spin ensemble was then allowed to relax according to Redfield's relaxation superoperator theory [51,52,54,55]; for the sake of simplicity the nuclear coordinates were chosen fixed in this exchange model, with values representative of what numerous random walks simulations yielded as average of the full volumes of the A and B configurations. Table I presents these prototypical proton and electron Cartesian coordinates, as well as additional parameters used to create the relevant spin Hamiltonian. Notice that no electron relaxation arising from inter-radical dipolar interactions are here considered; if present, these could be prevented by lowering the polarizing agent concentrations [11,56].

III. THE MF-JDNP EFFECT

While ODNP/JDNP propose to polarize nuclei by taking electron spins out of equilibrium via microwave irradiation, MF-JDNP attempts to polarize nuclei without microwaves. Instead, it exploits the temporary imbalance that will occur in the electron polarization, if samples are suddenly moved along the axis of a finite solenoid magnet. We hypothesize that if such non-equilibrated electronic spin state encounters the JDNP condition, the resulting relaxation process will lead to an imbalance between the α and β nuclear components of the singlet and the triplet state and in turn to NMR hyperpolarization. To explore this possibility numerous scenarios were envisioned; for simplicity we consider solely the one schematized in Fig. 2. Here the sample is repeatedly shuttled between a high field (14.1 T, corresponding to a 600 MHz ^{1}H Larmor frequency) where NMR measurements will be taken, and a field where the $J_{ex} \approx \pm\omega_E$ condition is fulfilled (in this case 9.1 T, corresponding to a $\omega_E \approx J_{ex} \approx -255$ GHz [37–39]). Considering that contemporary pneumatic shuttling setups can displace small samples with velocities of ≈ 40 m/s [57], and that the distance between the two positions in question for the field profile of a conventional superconducting NMR magnet is about 35 cm [41,45], constant shuttling rates of 0.25 T/ms were assumed.

Figures 3(a) and 3(b) show the consequence of the ensuing shuttling on the nuclear polarization, for a three-spin system. The parameters of these calculations are as given in Table I, with and without assuming exchanges between proton configurations A and B, respectively. The left-hand column in Fig. 3 shows the enhancements over the thermal nuclear polarization that will be achieved in each case from such experiment; the center column clarifies this further, by showing the fate of the various spin states that add up to the total nuclear polarization $\hat{N}_Z$ throughout the process. The right-hand column summarizes the physics of these events, by depicting the differential behavior of the various $\hat{T}_{\pm1,\beta/\alpha}$, $\hat{T}_{0,\beta/\alpha}$, and $\hat{S}_{0,\beta/\alpha}$ operators describing the triplet and singlet electronic coupled to the β/α nuclear-spin states.

At the crux of the proposal lie shuttling speeds that, even if leading to magnetic-field change rates that are still considerably slower than the Redfield relaxation rates of the

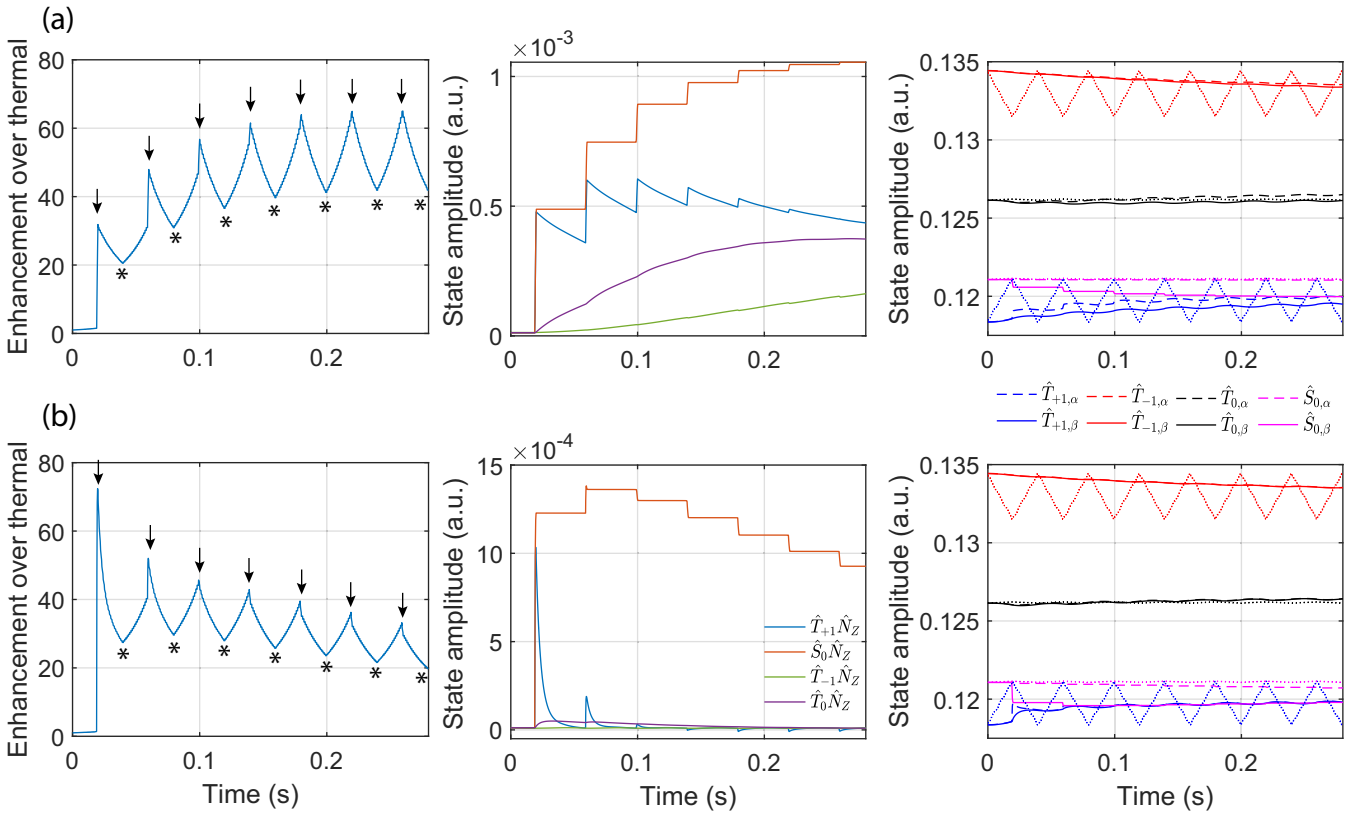

FIG. 3. MF-JDNP performed according to the scheme in Fig. 2, with $n = 7$ loops between an NMR field of 14.1 T, and a 9.1 T polarizing field fulfilling the JDNP condition. (a) Simulations assuming a three-spin system where the solvent proton exchanges between configurations A and B (Fig. 1). (b) Simulations assuming that the solvent proton was fixed in configuration A. In neither case were intra-radical protons considered. Left-hand column: Time (magnetic-field) evolution of the nuclear enhancement, scaled over the instantaneous thermal equilibrium magnetization value at each magnetic field. Black arrows indicate the JDNP condition; asterisks indicate NMR observation points. Center column: Time (magnetic-field) evolution of the $\hat{S}_0\hat{N}_Z$, $\hat{T}_0\hat{N}_Z$ and $\hat{T}_{\pm1}\hat{N}_Z$ states arising from the population imbalance between the α and β nuclear components of the singlet and triplet states; the sum of all these states corresponds to nuclear polarization scaled over the thermal equilibrium value at each magnetic field shown in the left-hand column. Right-hand column: Time (magnetic-field) evolution of the $\hat{S}_{0,\alpha/\beta}$, $\hat{T}_{0,\alpha/\beta}$, and $\hat{T}_{\pm1,\alpha/\beta}$ states (straight and dashed lines, respectively) compared to their thermal equilibrium values (dotted lines; the α and β nuclear components overlap).

electronic triplet states, are sufficiently fast for taking these states slightly out of the thermal equilibrium. These perturbances are illustrated in the right-hand column of Fig. 3, which compares the actual values of the above-mentioned states (with the straight and dashed lines representing the nuclear β/α states) vs their thermal equilibrium values (dotted lines). As these perturbed systems reach the JDNP condition, spectral densities reignite cross-relaxation processes between the $\hat{T}_{+1,\beta/\alpha}$ and $\hat{S}_{0,\beta/\alpha}$ states, which at other fields were too inefficient due to the large energy gap introduced by J_{ex}. The rates of these cross-relaxation processes depend on the ^{1}H spin state, resulting in a temporary imbalance between the α and β nuclear components associated with the triplet and, in particular, with the singlet states. The process that leads to this imbalance can be appreciated from Eqs. (S1)–(S5) in the Supplemental Material [47], which represent the relaxation rates of the α and β nuclear components of the electronic singlet and triplet states. These equations predict that for the symmetric biradicals being here considered, singlet self-relaxation rates will be dominated by the $(\Delta^2_{\Delta\text{HF}}/30)J(J_{\text{ex}} + \omega_E + \omega_N)$ term for $\hat{S}_{0,\beta}$, and by $(\Delta^2_{\Delta\text{HF}}/30)J(J_{\text{ex}} - \omega_E - \omega_N)$ for $\hat{S}_{0,\alpha}$, where $\Delta^2_{\Delta\text{HF}}$ is the second-rank norm squared arising from anisotropies associated with the difference between the dipolar hyperfine coupling tensors between the protons and the two electrons, $J(\omega)$ denotes the spectral density at frequency ω, and ω_E and ω_N are the electron and the nuclear Larmor frequencies, respectively. A negative $J_{\text{ex}} \approx \omega_E$ thus leads to $-R[\hat{S}_{0,\beta}] \gg -R[\hat{S}_{0,\alpha}]$, while a positive $J_{\text{ex}} \approx -\omega_E$ leads to $-R[\hat{S}_{0,\alpha}] \gg -R[\hat{S}_{0,\beta}]$. In either case a difference between the self-relaxation rates of $\hat{S}_{0,\alpha}$ and $\hat{S}_{0,\beta}$ leads to a population imbalance, and hence the creation of a transient, net nuclear magnetization enhancement. Such imbalance is reflected by the creation of $\hat{S}_0\hat{N}_Z = \hat{S}_{0,\alpha} - \hat{S}_{0,\beta}$, $\hat{T}_0\hat{N}_Z = \hat{T}_{0,\alpha} - \hat{T}_{0,\beta}$, and $\hat{T}_{\pm1}\hat{N}_Z = \hat{T}_{\pm1,\alpha} - \hat{T}_{\pm1,\beta}$ states (Fig. 3, central column), and therefore by an overall nuclear magnetization enhancement given by $\hat{N}_Z = (\hat{S}_0\hat{N}_Z + \hat{T}_0\hat{N}_Z + \hat{T}_{\pm1}\hat{N}_Z)/2$.

Spatially speaking, the enhancement predicted by this repeated shuttling is relatively isotropic [30]; it is maximized each time the JDNP condition is fulfilled, but begins to decay as the sample departs from this condition. This explains the oscillations displayed by $\hat{N}_Z$ with the shuttling; oscillations which are magnified further when considering the equilibrium

nuclear polarization at each field (Fig. 3, left-hand column). Still, as the field where the JDNP condition is maximal will in general not correspond with a traditional NMR observation field, the MF-JDNP approach assumes an additional shuttling back to the homogeneous 14.1 T field region for a conventional NMR observation. While lowering the enhancement that could be achieved if remaining at the JDNP condition, a significant NMR enhancement is still predicted. It is also enlightening to compare Fig. 3(a), which assumes that the nuclear spin can diffuse in and out of the polarization sphere, with Fig. 3(b), which assumes the spin spends all of its time in the polarizing A region. In the latter case, the shuttling leads to a clearly higher initial JDNP effect; however, the faster spin relaxation characterizing these electron proximate nuclei also leads to a rapid loss of this nuclear enhancement as the sample travels to the NMR detection field. By contrast, the buildup in the former case is slower, but builds up to higher final values upon looping. It appears, therefore, that diffusive processes end up having positive effects on the proposed scheme.

The aforementioned predictions assumed a three-spin system. Figure 4(a) shows the expectations arising from MF-JDNP if considering a four-spin system, which includes the presence of an intra-radical proton residing (without exchange) in region C that is dipolar and scalar coupled to the electrons. The addition of this fourth spin will decrease the enhancement of the solvent ^{1}H by approximately an order of magnitude, as most of the electron polarization imbalance created by the shuttling is now captured by the proton that is closer to the biradical. At the same time, this ~ 80-fold polarization enhancement of the intra-radical ^{1}H will also be lost quickly, due to the high nuclear relaxation rates induced by the nearby electrons. On the other hand, replacing the intra-radical proton by deuterium leads to an increase of the radical's T_1 [58] and reinstates a sizable enhancement (Fig. 4(b), blue line) even if it is still $\approx 40\%$ smaller than in the absence of any radical-based nucleus.

A final, important ingredient that may define the success or failure of the MF-JDNP strategy, concerns the presence of additional electronic spin-lattice relaxation processes; in particular, of relaxation mechanisms other than those treated by the Redfield model. For example, both for the case of trityl and of nitroxide-based monoradicals (and presumably for their biradicals as well), vibrational modes coupling the spins with orbital angular-momenta fluctuations, are known to lead to substantial decreases in the electron spin-relaxation times [58]. The magnitude of these relaxation rates can be high, reaching into 10^4 and 10^6 Hz for trityls and nitroxides, respectively [59–61]. Further, these effects are at the moment virtually impossible to calculate accurately from first principle, even if they can be inferred from vibrational measurements. These vibrational modulations may or may not interact with a biradical's singlet state, but will in all likelihood lead to significant changes in the $\hat{T}_{\pm 1,\alpha/\beta}$'s relaxation times, bringing them down to the $\approx$ µs range (see Supplemental Material for more details [47]). This could profoundly affect the MF-JDNP experiment, as illustrated in Fig. 4(b) for the case of a four-spin system that is now affected by vibrations-driven relaxation modes whose magnitude were estimated based on reports for monotrityl radicals [58,60,61]. Not surprisingly, the addition of such strong competing relaxation mechanism will cancel out almost entirely the polarization enhancement effects in the solvent expected from the MF-JDNP methodology (Fig. 4(b), violet trace).

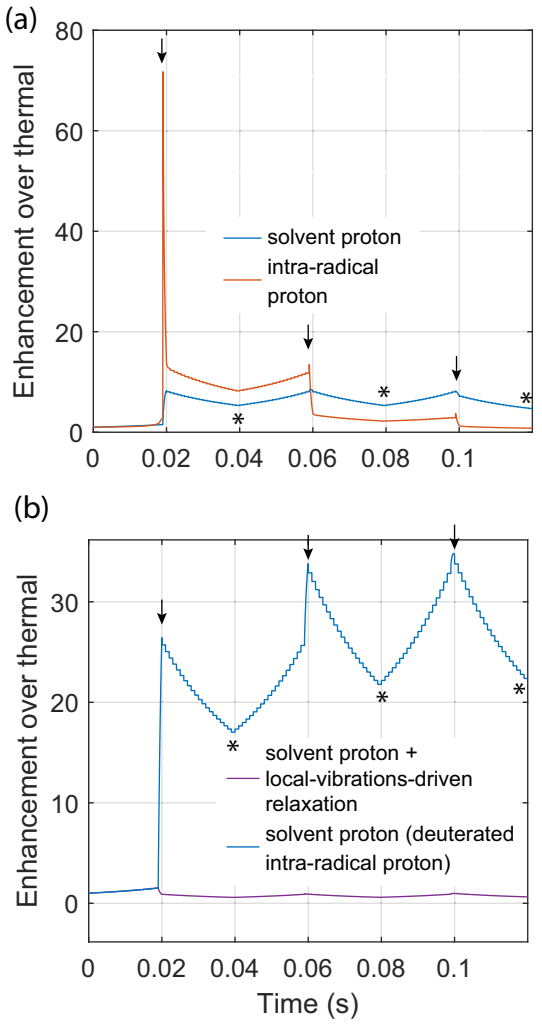

FIG. 4. Expectations of MF-JDNP experiments performed according to the scheme in Fig. 2, with three high-low-high B_0 shuttling repetitions. All plots show time (magnetic-field) evolution of the nuclear enhancement over the thermal equilibrium value. Black arrows indicate the JDNP condition; asterisks indicate potential NMR observation points. (a) Predictions for a four-spin system including a fixed intraradical proton (the electron-proton scalar coupling was set to 1 MHz) and a diffusion solvent. (b) The same as (a), but after replacing the intraradical proton by a deuterium (blue line) but including an *ad hoc* term in the Redfield relaxation superoperator, applied only to the electron longitudinal states, representing a 6×10^4 Hz local vibrations-driven contribution to the relaxation modes (violet line).

IV. DISCUSSION AND CONCLUSIONS

This study explored the possibility of combining the JDNP effect that will spontaneously transfer electron polarization to nearby nuclei under $J_{ex} \approx \pm\omega_E$ conditions, with rapid sample-field cycling. Exchange couplings on the order of several GHz have been reported for a number of biradicals using monophenyl, biphenyls, and acetylene linkers [39,62–64]. Pure hydrocarbon biradicals created using these

linkers are expected to be conformationally rigid [64], leading to a J_{ex} value that will remain constant during the JDNP nuclear polarization buildup (while modulation of J_{ex} due to putative conformational dynamics will not lead to shortening in the electron's state relaxation rates), thereby enabling the JDNP experiment [53]. The question now is how to use JDNP's potential, for enhancing NMR sensitivity at high magnetic fields without microwave irradiation. MF-JDNP could achieve this, by exploiting shuttling rates of $\approx$ T/ms in order to create a sufficient disturbance in the electron polarization; only under such conditions will an out-of-equilibrium situation be created in the absence of microwaves. Then, as the sample is cycled through fields that include fulfillment of the JDNP condition, nuclear polarization is spontaneously created. The present study assumed a lower field JDNP condition and shuttling back to higher field for NMR measurements; alternatives providing comparable nuclear enhancements while shuttling from lower NMR to higher JDNP-fulfilling fields, can also be devised.

All the scenarios that were here analyzed involved radicals whose electron relaxation times were dominated by dipolar hyperfine relaxation, and T_1s for the singlet and triplet states that are comparable to the shuttling times. Notice that as further discussed in the Supplemental Material [47] these triplet- and singlet relaxation rates can be orders of magnitude smaller than longitudinal T_1 electron relaxation rates, which reach in excess of $\approx 10^6$ Hz in biradicals at any magnetic field [60]. The presence of intra-radical protons can affect these rates and decrease the nuclear hyperpolarization of the solvent; however, this can be largely restored if the former are substituted by deuterons. Eventually, however, the presence of very strong competing relaxation mechanism like those stemming from local vibrational modes—arising in the case of trityls from the stretching of the C–S bonds in the radical structures—might shorten further the lifetimes of the above-mentioned states, eliminating the MF-JDNP effect altogether. These effects will arise from the mixing between spin and orbital angular momenta, as driven by spin-orbit coupling (SOC). Although detrimental for MF-JDNP, these SOCs can be suppressed by eliminating the heavy atoms (heavier than ^{19}F) from the biradical structure, thereby restoring sufficiently slow electron relaxation rates to support MF-JDNP [56,65]. Alternatives to bypass such electron relaxation mechanisms competing with Redfield relaxation are also important in spintronics, and therefore are actively being sought [56]. Additional electron relaxation mechanisms might arise due to vibrations and collisions with surrounding diamagnetic molecules [66]; however, these processes are not expected in biradicals that make weak intermolecular interactions with the solvent. The MF-JDNP experiment might thus be realized using deuterated carbon-centered hydrocarbon radical centers free from heteroatoms, linked by monophenyl or acetylene units [64]. From an instrumentation standpoint current-shuttling technologies could enable field disturbances on the order of ~ 0.25 T/ms [41,45], sufficient to enable the MF-JDNP effect. Tests based on these chemical and technological systems are currently in progress.

ACKNOWLEDGMENTS

This project was funded by The Israel Science Foundation (Grant No. ISF 965/18), the Minerva Foundation (Germany), and the US National Science Foundation (Grants No. CHE-2203405 and No. DMR-2128556). M.G.C. acknowledges Weizmann's Faculty of Chemistry for support by a Dean Fellowship. L.F. holds the Bertha and Isadore Gudelsky Professorial Chair and Heads the Clore Institute for High-Field Magnetic Resonance Imaging and Spectroscopy, whose support is acknowledged, as is the generosity of the Perlman Family Foundation. The authors acknowledge Professor Ilya Kuprov, Professor Olav Schiemann, and Mr. Kevin Kopp for discussions.

[1] A. W. Overhauser, Polarization of nuclei in metals, Phys. Rev. **92**, 411 (1953).

[2] T. R. Carver and C. P. Slichter, Experimental verification of the Overhauser nuclear polarization effect, Phys. Rev. **102**, 975 (1956).

[3] K. H. Hausser and D. Stehlik, Dynamic nuclear polarization in liquids, in *Advances in Magnetic and Optical Resonance* (Elsevier, Amsterdam, Netherlands, 1968), pp. 79–139.

[4] N. M. Loening, M. Rosay, V. Weis, and R. G. Griffin, Solution-state dynamic nuclear polarization at high magnetic field, J. Am. Chem. Soc. **124**, 8808 (2002).

[5] P. Hofer, G. Parigi, C. Luchinat, P. Carl, G. Guthausen, M. Reese, T. Carlomagno, C. Griesinger, and M. Bennati, Field dependent dynamic nuclear polarization with radicals in aqueous solution, J. Am. Chem. Soc. **130**, 3254 (2008).

[6] G. Q. Liu, M. Levien, N. Karschin, G. Parigi, C. Luchinat, and M. Bennati, One-thousand-fold enhancement of high field liquid nuclear magnetic resonance signals at room temperature, Nat. Chem. **9**, 676 (2017).

[7] G. Parigi, E. Ravera, M. Bennati, and C. Luchinat, Understanding overhauser dynamic nuclear polarisation through NMR relaxometry, Mol. Phys. **117**, 888 (2019).

[8] M. Levien, M. Hiller, I. Tkach, M. Bennati, and T. Orlando, Nitroxide derivatives for dynamic nuclear polarization in liquids: The role of rotational diffusion, J. Phys. Chem. Lett. **11**, 1629 (2020).

[9] M. Levien, M. Reinhard, M. Hiller, I. Tkach, M. Bennati, and T. Orlando, Spin density localization and accessibility of organic radicals affect liquid-state DNP efficiency, Phys. Chem. Chem. Phys. **23**, 4480 (2021).

[10] D. H. Dai, X. W. Wang, Y. W. Liu, X. L. Yang, C. Glaubitz, V. Denysenkov, X. He, T. Prisner, and J. F. Mao, Room-temperature dynamic nuclear polarization enhanced NMR spectroscopy of small biological molecules in water, Nat. Commun. **12**, 6880 (2021).

[11] J. H. Ardenkjaer-Larsen, I. Laursen, I. Leunbach, G. Ehnholm, L. G. Wistrand, J. S. Petersson, and K. Golman, EPR and DNP properties of certain novel single electron contrast agents intended for oximetric imaging, J. Magn. Reson. **133**, 1 (1998).

[12] R. A. Wind and J. H. Ardenkjaer-Larsen, ^{1}H DNP at 1.4 T of water doped with a triarylmethyl-based radical, J. Magn. Reson. **141**, 347 (1999).

[13] J. H. Ardenkjaer-Larsen, B. Fridlund, A. Gram, G. Hansson, L. Hansson, M. H. Lerche, R. Servin, M. Thaning, and K. Golman,

Increase in signal-to-noise ratio of >10,000 times in liquid-state NMR, Proc. Natl. Acad. Sci. USA **100**, 10158 (2003).

[14] K. Golman, M. Lerche, R. Pehrson, and J. H. Ardenkjaer-Larsen, Metabolic imaging by hyperpolarized 13C magnetic resonance imaging for in vivo tumor diagnosis, Cancer Res. **66**, 10855 (2006).

[15] J. H. Ardenkjaer-Larsen, G. S. Boebinger, A. Comment, S. Duckett, A. S. Edison, F. Engelke, C. Griesinger, R. G. Griffin, C. Hilty, H. Maeda, G. Parigi, T. Prisner, E. Ravera, J. van Bentum, S. Vega, A. Webb, C. Luchinat, H. Schwalbe, and L. Frydman, Facing and overcoming sensitivity challenges in biomolecular NMR spectroscopy, Angew. Chem. Int. Ed. Engl. **54**, 9162 (2015).

[16] T. Dubroca, S. Wi, J. van Tol, L. Frydman, and S. Hill, Large volume liquid state scalar Overhauser dynamic nuclear polarization at high magnetic field, Phys. Chem. Chem. Phys. **21**, 21200 (2019).

[17] D. Yoon, A. I. Dimitriadis, M. Soundararajan, C. Caspers, J. Genoud, S. Alberti, E. de Rijk, and J. P. Ansermet, High-field liquid-state dynamic nuclear polarization in microliter samples, Anal. Chem. **90**, 5620 (2018).

[18] T. Dubroca, A. N. Smith, K. J. Pike, S. Froud, R. Wylde, B. Trociewitz, J. Mckay, F. Mentink-Vigier, J. van Tol, S. Wi, W. Brey, J. R. Long, L. Frydman, and S. Hill, A quasi-optical and corrugated waveguide microwave transmission system for simultaneous dynamic nuclear polarization NMR on two separate 14.1 T spectrometers, J. Magn. Reson. **289**, 35 (2018).

[19] W. Mullerwarmuth and K. Meisegresch, Molecular motions and interactions as studied by dynamic nuclear-polarization (DNP) in free-radical solutions, Adv. Magn. Reson. **11**, 1 (1983).

[20] C. Griesinger, M. Bennati, H. M. Vieth, C. Luchinat, G. Parigi, P. Höfer, F. Engelke, S. J. Glaser, V. Denysenkov, and T. F. Prisner, Dynamic nuclear polarization at high magnetic fields in liquids, Prog. Nucl. Magn. Reson. Spectrosc. **64**, 4 (2012).

[21] T. Orlando, I. Kuprov, and M. Hiller, Theoretical analysis of scalar relaxation in ^{13}C-DNP in liquids, JMRO **10-11**, 100040 (2022).

[22] K. H. Hausser and D. Stehlik, Dynamic nuclear polarization in liquids, in *Advances in Magnetic and Optical Resonance* (Elsevier, Amsterdam, 1968).

[23] T. Prisner, V. Denysenkov, and D. Sezer, Liquid state DNP at high magnetic fields: Instrumentation, experimental results and atomistic modelling by molecular dynamics simulations, J. Magn. Reson. **264**, 68 (2016).

[24] E. Ravera, C. Luchinat, and G. Parigi, Basic facts and perspectives of Overhauser DNP NMR, J. Magn. Reson. **264**, 78 (2016).

[25] M. Soundararajan, T. Dubroca, J. Van Tol, S. Hill, L. Frydman, and S. Wi, Proton-detected solution-state NMR at 14.1 T based on scalar-driven ^{13}C Overhauser dynamic nuclear polarization, J. Magn. Reson. **343**, 107304 (2022).

[26] K.-N. Hu, H.-H. Yu, T. M. Swager, and R. G. Griffin, Dynamic nuclear polarization with biradicals, J. Am. Chem. Soc. **126**, 10844 (2004).

[27] V. S. Bajaj, M. K. Hornstein, K. E. Kreischer, J. R. Sirigiri, P. P. Woskov, M. L. Mak-Jurkauskas, J. Herzfeld, R. J. Temkin, and R. G. Griffin, 250 GHz CW gyrotron oscillator for dynamic nuclear polarization in biological solid state NMR, J. Magn. Reson. **189**, 251 (2007).

[28] K. N. Hu, G. T. Debelouchina, A. A. Smith, and R. G. Griffin, Quantum mechanical theory of dynamic nuclear polarization in solid dielectrics, J. Chem. Phys. **134**, 125105 (2011).

[29] V. Bajaj, C. Farrar, M. Hornstein, I. Mastovsky, J. Vieregg, J. Bryant, B. Elena, K. Kreischer, R. Temkin, and R. Griffin, Dynamic nuclear polarization at 9 T using a novel 250 GHz gyrotron microwave source, J. Magn. Reson. **213**, 404 (2011).

[30] M. G. Concilio, I. Kuprov, and L. Frydman, J-Driven dynamic nuclear polarization for sensitizing high field solution state NMR, Phys. Chem. Chem. Phys. **24**, 2118 (2022).

[31] J. Bargon, H. Fischer, and U. Johnsen, Kernresonanz-Emissionslinien während rascher Radikalreaktionen, Z. Naturforsch. A **22**, 1551 (1967).

[32] G. L. Closs, A mechanism explaining nuclear spin polarizations in radical combination reactions, J. Am. Chem. Soc. **91**, 4552 (1969).

[33] R. Kaptein and J. L. Oosterhoff, Chemically induced dynamic nuclear polarization II - (Relation with anomalous ESR spectra), Chem. Phys. Lett. **4**, 195 (1969).

[34] R. Kaptein, P. W. N. M. Vanleeuwen, and R. Huis, S-T$^{\pm}$ CIDNP from a thermally-generated biradical, Chem. Phys. Lett. **41**, 264 (1976).

[35] F. J. J. D. Kanter, R. Kaptein, and R. A. Vansanten, Magnetic-field dependent biradical CIDNP as a tool for study of conformations of polymethylene chains, Chem. Phys. Lett. **45**, 575 (1977).

[36] P. J. Hore and R. W. Broadhurst, Photo-CIDNP of biopolymers, Prog. NMR Spectrosc. **25**, 345 (1993).

[37] J. J. Jassoy, A. Meyer, S. Spicher, C. Wuebben, and O. Schiemann, Synthesis of nanometer sized bis- and tris-trityl model compounds with different extent of spin-spin coupling, Molecules **23**, 682 (2018).

[38] G. W. Reginsson, N. C. Kunjir, S. T. Sigurdsson, and O. Schiemann, Trityl radicals: Spin labels for nanometer-distance measurements, Chem. Eur. J. **18**, 13580 (2012).

[39] N. Fleck, T. Hett, J. Brode, A. Meyer, S. Richert, and O. Schiemann, C-C cross-coupling reactions of trityl radicals: Spin density delocalization, exchange coupling, and a spin label, J. Org. Chem. **84**, 3293 (2019).

[40] M. Reese, D. Lennartz, T. Marquardsen, P. Hofer, A. Tavernier, P. Carl, T. Schippmann, M. Bennati, T. Carlomagno, F. Engelke, and C. Griesinger, Construction of a liquid-state NMR DNP shuttle spectrometer: First experimental results and evaluation of optimal performance characteristics, Appl. Magn. Reson. **34**, 301 (2008).

[41] M. Reese, M. T. Turke, I. Tkach, G. Parigi, C. Luchinat, T. Marquardsen, A. Tavernier, P. Hofer, F. Engelke, C. Griesinger, and M. Bennati, H-1 and C-13 dynamic nuclear polarization in aqueous solution with a two-field (0.35 T/14 T) shuttle DNP sspectrometer, J. Am. Chem. Soc. **131**, 15086 (2009).

[42] R. Fischer, C. O. Bretschneider, P. London, D. Budker, D. Gershoni, and L. Frydman, Bulk Nuclear Polarization Enhanced at Room Temperature by Optical Pumping, Phys. Rev. Lett. **111**, 057601 (2013).

[43] P. J. M. van Bentum, M. Sharma, S. G. J. van Meerten, and A. P. M. Kentgens, Solid effect DNP in a rapid-melt setup, J. Magn. Reson. **263**, 126 (2016).

[44] S. G. J. van Meerten, G. E. Janssen, and A. P. M. Kentgens, Rapid-melt DNP for multidimensional and heteronuclear high-field NMR experiments, J. Magn. Reson. **310**, 106656 (2020).

[45] A. Krahn, P. Lottmann, T. Marquardsen, A. Tavernier, M. T. Turke, M. Reese, A. Leonov, M. Bennati, P. Hoefer, F. Engelke, and C. Griesinger, Shuttle DNP spectrometer with a two-center magnet, Phys. Chem. Chem. Phys. **12**, 5830 (2010).

[46] H. J. Hogben, M. Krzystyniak, G. T. P. Charnock, P. J. Hore, and I. Kuprov, Spinach–A software library for simulation of spin dynamics in large spin systems, J. Magn. Reson. **208**, 179 (2011).

[47] See Supplemental Material at http://link.aps.org/supplemental/10.1103/PhysRevE.107.035303 for the simulation and proton random-walk codes used in the present analysis, singlet and triplet relaxation rates for the intraradical protons, numerical singlet and triplet relaxation rates as a function of the magnetic field, and the effect of g-tensor orientation on the enhancement, which includes Refs. [30,58–60,67].

[48] S. Vega, Fictitious spin 1/2 operator formalism for multiple quantum NMR, J. Chem. Phys. **68**, 5518 (1978).

[49] R. R. Ernst, G. Bodenhausen, and A. Wokaun, *Principles of Nuclear Magnetic Resonance in One and Two Dimensions* (Clarendon Press, Oxford, 1987).

[50] A. Redfield, The theory of relaxation processes, in *Advances in Magnetic and Optical Resonance* (Elsevier, Amsterdam, Netherlands, 1965).

[51] M. Goldman, Formal theory of spin-lattice relaxation, J. Magn. Reson. **149**, 160 (2001).

[52] I. Kuprov, N. Wagner-Rundell, and P. Hore, Bloch-Redfield-Wangsness theory engine implementation using symbolic processing software, J. Magn. Reson. **184**, 196 (2007).

[53] I. Kuprov, D. M. Hodgson, J. Kloesges, C. I. Pearson, B. Odell, and T. D. Claridge, Anomalous nuclear Overhauser effects in carbon-substituted aziridines: Scalar cross-relaxation of the first kind, Angew. Chem. Int. Ed. **54**, 3697 (2015).

[54] M. H. Levitt and L. Dibari, Steady-State in Magnetic-Resonance Pulse Experiments, Phys. Rev. Lett. **69**, 3124 (1992).

[55] D. Goodwin and I. Kuprov, Auxiliary matrix formalism for interaction representation transformations, optimal control, and spin relaxation theories, J. Chem. Phys. **143**, 084113 (2015).

[56] S. Schott, E. R. McNellis, C. B. Nielsen, H. Y. Chen, S. Watanabe, H. Tanaka, I. McCulloch, K. Takimiya, J. Sinova, and H. Sirringhaus, Tuning the effective spin-orbit coupling in molecular semiconductors, Nat. Commun. **8**, 15200 (2017).

[57] V. Biancalana, Y. Dancheva, and L. Stiaccini, Note: A fast pneumatic sample-shuttle with attenuated shocks, Rev. Sci. Instrum. **85**, 036104 (2014).

[58] L. Yong, J. Harbridge, R. W. Quine, G. A. Rinard, S. S. Eaton, G. R. Eaton, C. Mailer, E. Barth, and H. J. Halpern, Electron spin relaxation of triarylmethyl radicals in fluid solution, J. Magn. Reson. **152**, 156 (2001).

[59] R. Owenius, G. R. Eaton, and S. S. Eaton, Frequency (250 MHz to 9.2 GHz) and viscosity dependence of electron spin relaxation of triarylmethyl radicals at room temperature, J. Magn. Reson. **172**, 168 (2005).

[60] H. Sato, V. Kathirvelu, G. Spagnol, S. Rajca, A. Rajca, S. S. Eaton, and G. R. Eaton, Impact of electron-electron spin interaction on electron spin relaxation of nitroxide diradicals and tetraradical in glassy solvents between 10 and 300 K, J. Phys. Chem. B **112**, 2818 (2008).

[61] A. A. Kuzhelev, D. V. Trukhin, O. A. Krumkacheva, R. K. Strizhakov, O. Y. Rogozhnikova, T. I. Troitskaya, M. V. Fedin, V. M. Tormyshev, and E. G. Bagryanskaya, Room-temperature electron spin relaxation of triarylmethyl radicals at the X- and Q-bands, J. Phys. Chem. B **119**, 13630 (2015).

[62] O. I. Gromov, E. N. Golubeva, V. N. Khrustalev, T. Kalai, K. Hideg, and A. I. Kokorin, EPR, the x-ray structure and DFT calculations of the nitroxide biradical with one acetylene group in the bridge, Appl. Magn. Reson. **45**, 981 (2014).

[63] A. I. Kokorin, Regularities of the spin exchange coupling through a bridge in nitroxide biradicals, Appl. Magn. Reson. **26**, 253 (2004).

[64] H. H. Haeri, P. Spindler, J. Plackmeyer, and T. Prisner, Double quantum coherence ESR spectroscopy and quantum chemical calculations on a BDPA biradical, Phys. Chem. Chem. Phys. **18**, 29164 (2016).

[65] I. V. Khudyakov, Y. A. Serebrennikov, and N. J. Turro, Spin-orbit-coupling in free-radical reactions - on the way to heavy-elements, Chem. Rev. **93**, 537 (1993).

[66] D. Kivelson, Electric-field fluctuations and spin relaxation in liquids, J. Chem. Phys. **45**, 1324 (1966).

[67] D. M. Brink and G. R. Satchler, *Angular Momentum*, 3rd ed. (Oxford University Press, Oxford, UK, 1994).